Biochimica et Biophysica Acta, 636 (1981) 50–57
Elsevier/North-Holland Biomedical Press

BBA 48061

THE EFFECT OF TEMPERATURE AND TRANSMEMBRANE POTENTIALS ON THE RATES OF ELECTRON TRANSFER BETWEEN MEMBRANE-BOUND BIOLOGICAL REDOX COMPONENTS

A.M. KUZNETSOV [a] and J. ULSTRUP [b]

[a] *Institute of Electrochemistry, Academy of Sciences of the U.S.S.R., Leninskij Prospect 31, Moscow V-71 (U.S.S.R.) and* [b] *Chemistry Department A, Building 207, The Technical University of Denmark, 2800 Lyngby (Denmark)*

(Received October 17th, 1980)

Key words: *Electron transfer; Membrane potential; Temperature effect; Bacterial photosynthesis; Quantum-mechanical rate theory*

We have investigated rate data for the temperature and free energy dependence of the primary electron-transfer processes in bacterial photosynthesis. Rather than representing the whole electronic-nuclear coupling by a frequently applied discrete single-mode model, we have incorporated a continuum of modes characterized by a certain distribution function. In this way, we can illuminate the role of both a broad distribution of low-frequency modes representing the medium and a narrow distribution representing local nuclear modes. Furthermore, it emerges from the calculations that both sets are important in the overall scheme of primary photosynthetic electron-transfer processes. By means of this model and quantum-mechanical rate theory, we can reproduce a number of important features of the primary photosynthetic processes concerning in particular the temperature (tunnelling or thermally activated nuclear motion) and free energy dependence ('normal', 'activationless', or 'inverted' regions) of the rate constants and estimate such parameters as nuclear-reorganization energy, electron-exchange integrals and electron-transfer distances. We have finally considered some of the important factors which determine the potential drop across the membrane and estimated the extent to which variations in the potential drop affect the rate constants of the electron-transfer processes.

Introduction

The sequence of primary electron-transfer steps in bacterial photosynthesis is believed to be represented by the following scheme [1–3]:

$$(BChl)_2^* + BPh \rightarrow (BChl)_2^+ + BPh^-$$

$\tau_{1/2} \approx 10$ ps [4–7] 0.35–0.55 eV (1)

$$BPh^- + A_1 \rightarrow BPh + A_1^-$$

$\tau_{1/2} \approx 1$–200 ps [4–7] 0.22–0.44 eV (2)

$$\text{cytochrome } c^{II} + (BChl)_2^+ \rightarrow \text{cytochrome } c^{III} + (BChl)_2$$

$\tau_{1/2} \approx 1\ \mu s$ [8–14] 0.5 eV (3)

$$A_1^- + A_2 \rightarrow A_1 + A_2^-$$

$\tau_{1/2} \approx 0.2$–0.4 ms [15–17] 0.06 eV (4)

where the columns to the right give the room temperature half-lives and energy gaps [2,18] (negative free energy differences as determined by the standard redox potentials of the redox couples involved). $(BChl)_2$ is the reaction centre bacteriochlorophyll dimer, $(BChl)_2^*$ its first excited singlet state from which the photoexcited electron is transferred to bacteriopheophytin, BPh, and A_1 and A_2 the 'primary' and 'secondary' quinone electron acceptors. If the forward electron transfer is blocked by reduction or extraction of the quinones, the reduced ground state $(BChl)_2$ is regenerated by the following relatively slow electron transfer steps:

Abbreviations: BChl, bacteriochlorophyll; BPh, bacteriopheophytin.

$$(BChl)_2^+ + BPh^- \rightarrow (BChl)_2 + BPh$$

$$\tau_{1/2} \approx 10\text{–}30 \text{ ns } [19,20] \quad 0.85\text{–}1.05 \text{ eV} \quad (5)$$

$$^1[(BChl)_2^+ + BPh^-] \rightarrow {}^3[(BChl)_2^+ + BPh^-]$$

$$\tau_{1/2} \approx 10 \text{ ns} \quad (6a)$$

$$^3[(BChl)_2^+ + BPh^-] \rightarrow {}^3(BChl)_2^* + BPh$$

$$\tau_{1/2} \approx 10 \text{ ns} \quad 0.2 \text{ eV} \quad (6b)$$

$$(BChl)_2^+ + A_1^- \rightarrow (BChl)_2 + A_1$$

$$\tau_{1/2} \approx 10\text{–}100 \text{ ms } [3,9\text{–}14] \quad 0.6 \text{ eV} \quad (7)$$

Reaction 5 represents electron transfer from BPh^- to the ground state of $(BChl)_2$, while reactions 6a and 6b involve magnetic interactions of the unpaired electrons in the radical pair $^1[(BChl)_2^+ + Bph^-]$ with the nuclei to form the triplet pair which subsequently decays to the excited triplet $^3(BChl)_2$ [19–23]. A detailed model for this exchange interaction based on studies of electron transfer at electrolyte/organic crystal interphases was recently reported [24] (cf. also Ref. 25).

The physical nature of reactions 1–7 has attracted considerable interest recently in the light of quantum-mechanical rate theory. Attention has thus been given to:

(a) The different temperature dependence of the reactions. Reactions 1 and 2 are temperature independent right down to cryogenic temperatures, and the rate of reaction 7 even decreases slightly with increasing temperature, T, when $T \gtrsim 150$ K, while it is practically constant at lower temperatures ($\tau_{1/2}$ decreases from about 60 ms at 300 K to about 20 ms at 80 K for the species *Rhodopseudomonas Sphaeroides*. In contrast, reaction 3 is temperature independent for $T \lesssim 100$ K ($\tau_{1/2} = 2\text{–}3$ ms), while it follows an Arrhenius dependence of activation energy 0.1–0.2 eV at higher temperatures [8–14]. Reaction 4 apparently displays similar behaviour where, however, the transition temperature is about 200 K [16,17]. Finally, reaction 5 shows a weak rate increase with increasing T, $\tau_{1/2}$ falling from about 20 ns at 20 K to about 6 ns at room temperature [19].

(b) The magnetic interactions in reactions 6a and 6b resulting in the formation of triplet $^3(BChl)_2^*$ in magnetic field-dependent yields. The yield also increases from 10–20% at room temperature, indicating a dominating contribution of reaction 5 to the decay of $^1[(BChl)_2^+ + BPh^-]$, to 100% at 20 K 19,20].

Several temperature effects of the individual processes are basically understandable from recent formulations of quantum-mechanical electron-transfer theory using models in which the whole electronic-vibrational coupling is represented by a single pair of displaced harmonic oscillators for the nuclear potential energy surfaces [26–28]. However, a closer inspection of the rates of reactions 1–7 shows that this coupling should be represented by a more detailed description [29,30]. In the following we shall therefore consider the temperature and free energy dependence of the rate constants for electron-transfer systems in which the electron is coupled not only to local nuclear modes (such as metal-ligand vibrations in transition metal complexes or C-C skeletal modes in organic radical ions), but also to a broad continuum of low-frequency modes, corresponding to relaxational motion, hydrogen-bond deformation, etc., in the membrane or external medium. Moreover, while the temperature is an external variable which can be varied over wide ranges, free energy variation for the membrane-bound molecules is restricted to comparison between different electron-transfer reactions or the small variations in the redox potentials which might be induced by external transmembrane potential differences. On the basis of our numerical free energy relationships, we shall therefore also estimate the possible effect of transmembrane potential variation on the electron-transfer rate constants.

Temperature effect on the electron-transfer rate constants

We shall consider electronic-vibrational coupling between the electron donor and acceptor sites and a continuous distribution of nuclear modes characterized by a 'reorganization energy density', $\epsilon_r(\omega)$, at the frequency, ω, related to the total nuclear reorganization energy, E_r, by [31]:

$$\int_0^\infty d\omega \, \epsilon_r(\omega) = E_r \quad (8)$$

The coupling is assumed to be linear. For discrete nuclear modes this corresponds to displaced harmonic

nuclear potential surfaces. For electrostatic coupling to a continuous medium it means that the polarization is proportional to the vacuum electric field of the molecular charge distribution. The rate expression is then:

$$W = \frac{\beta L^2}{i\hbar} \int_{-i\infty}^{i\infty} d\theta \exp[-\beta\Delta E - \Phi(\theta)]; \quad \beta = (k_B T)^{-1} \tag{9}$$

where L is a two-centre electron-transfer integral, k_B Boltzmann's constant, $\hbar$ Planck's constant divided by 2π, ΔE the free energy of reaction (energy gap), and the function $\Phi(\theta)$:

$$\Phi(\theta) = \frac{2}{\hbar} \int_0^\infty \frac{d\omega}{\omega} \epsilon_r(\omega) \frac{\text{sh}\frac{\beta\hbar\omega}{2}\theta \,\text{sh}\frac{\beta\hbar\omega}{2}(1-\theta)}{\text{sh}\frac{\beta\hbar\omega}{2}} \tag{10}$$

In the limit of strong coupling, and if we can take the upper limit for the integration with respect to ω as the threshold for electronic absorption, Eq. 9 can be calculated by the saddle-point method (cf. Ref. 32)

$$W = \frac{\beta L^2}{\hbar} \left\{ \frac{1}{2\pi} |\Phi''(\theta^*)| \right\}^{-1/2} \exp[-\beta\theta^*\Delta E - \Phi(\theta^*)] \tag{11}$$

where $\Phi''(\theta^*)$ is the second derivative of $\Phi(\theta)$ with respect to θ at the saddle point θ^*. The latter is determined by the equation:

$$\Delta E = \int_0^\infty d\omega \epsilon_r(\omega) \frac{\text{sh}\frac{\beta\hbar\omega}{2}(2\theta^* - 1)}{\text{sh}\frac{\beta\hbar\omega}{2}} \tag{12}$$

The condition for the prevalence of the strong-coupling limit and the applicability of the saddle-point method is, for a broad distribution [31]:

$$E_r/\hbar\omega_m >> 1 (\beta\hbar\omega_m >> 1);$$
$$2E_r/\beta(\hbar\omega_m)^2 >> 1 (\beta\hbar\omega_m << 1) \tag{13}$$

where ω_m is the maximum of the distribution. For a narrow distribution of width Γ ($\Gamma < \omega_m$, cf. Eqn. 19), the left-hand side of the inequalities of Eqn. 13 must be modified by the factor Γ/ω_m.

Eqs. 9–12 provide a prescription for the numerical calculation of the rate constant for given values of ΔE, T and the frequency dispersion function. In particular, for temperatures higher than a critical value $T_{cr} \approx \hbar\omega_m/2k_B$, the hyperbolic sine functions can be replaced by their arguments to give the usual high-temperature rate expression [32–40]:

$$W = L^2(\beta\pi/\hbar^2 E_r)^{1/2} \exp[-\beta(E_r + \Delta E)^2/4E_r] \tag{14}$$

Except for a single-mode approximation, analogous simple expressions are only available in certain cases below the critical temperature. A single mode of frequency ω_0 corresponds to $\epsilon_r = 1/2\hbar\omega_0\Delta^2\delta(\omega - \omega_0)$, where Δ is the reduced coordinate displacement [33–39]. Eqn. 9 can then be converted to the result obtained previously in different contexts [27,33–36,38–40]:

$$W = A \exp[-\tfrac{1}{2}\Delta^2(2\bar{\nu}+1)] I_p\{[\Delta^2\bar{\nu}(\bar{\nu}+1)]^{1/2}\} \times [(\bar{\nu}+1)/\bar{\nu}]^{p/2} \tag{15a}$$

$$\bar{\nu} = [\exp(\hbar\omega_0/k_B T) - 1]^{-1}; \quad A = 2\pi L^2/\hbar^2\omega_0 \tag{15b}$$

where $I_p(x)$ is the modified Bessel function of order p ($p = |\Delta E|/\hbar\omega_0$). In the low-temperature limit, this becomes (cf. Ref. 40):

$$W = A \exp(-\tfrac{1}{2}\Delta^2)(\tfrac{1}{2}\Delta^2)^p/p! \tag{16}$$

W/A coincides with the nuclear Franck Condon overlap factor of the harmonic oscillator wave functions of the ground initial and p-th excited final state vibrational levels [41]. In this limit, the nuclear reorganization thus proceeds in an activationless fashion by nuclear tunnelling between these two levels. For a broad continuum, a corresponding expression (for $p = 0$) is found by noting that for $\Delta E = 0$ (a 'symmetric' reaction) Eqn. 12 has the exact solution $\theta^* = 0.5$. In this case:

$$W = \frac{L^2}{\hbar}\left\{\frac{1}{2\pi}\hbar \int_0^\infty \frac{\omega\epsilon_r(\omega)\,d\omega}{\text{sh}\frac{\beta\hbar\omega}{2}}\right\}^{-1/2} \times \exp\left[-\frac{2}{\hbar}\int_0^\infty \frac{d\omega}{\omega}\epsilon_r(\omega)\,\text{th}(\beta\hbar\omega/4)\right] \tag{17}$$

In the low-temperature limit $\text{th}(\beta\hbar\omega/4) \to 1$, and the exponential factor reflects the nuclear tunnelling between the ground vibrational levels in the initial and final electronic states.

We shall finally need a representation of $\epsilon_r(\omega)$.

If the nuclear motion corresponds to a relaxation via an energy barrier, the distribution of oscillators is commonly represented by a Debye function [31]:

$$\epsilon_r(\omega) = (2E_r\Omega_D/\pi)(\Omega_D^2 + \omega^2)^{-1} \tag{18}$$

where Ω_D is the Debye frequency. This is a good representation for the major contribution to E_r for electron transfer at room temperature [42–44]. However, in view of the different nature of the membrane structure we shall represent $\epsilon_r(\omega)$ as a single resonance function or an overlap of resonances:

$$\frac{\epsilon_r(\omega)}{E_r} = \sum_i \frac{n_i\Gamma_i(\Omega_{Ri}^2 + \Gamma_i^2)}{[(\Omega_{Ri} - \omega)^2 + \Gamma_i^2][(\Omega_{Ri} + \omega)^2 + \Gamma_i^2]}$$

$$\left\{\sum_i \int_0^\infty \frac{n_i\Gamma_i(\Omega_{Ri}^2 + \Gamma_i^2)\,d\omega}{[(\Omega_{Ri} - \omega)^2 + \Gamma_i^2][(\Omega_{Ri} + \omega)^2 + \Gamma_i^2]}\right\}^{-1} \tag{19}$$

where Ω_{Ri} ($i = 1, 2$) is the frequency of the i-th resonance, Γ_i the width, and n_i a measure of the relative contribution of the i-th resonance. This corresponds to elastic deformation of the particular oscillators from their equilibrium positions [42], and we shall invoke a relatively narrow ($\Gamma \approx 50$ cm^{-1}) resonance of high frequency ($\Omega_{Ri} \gtrsim 400$ cm^{-1}, or $\Gamma/\Omega_R = 0.1$–0.2) to represent a discrete mode and a broad resonance ($\Gamma \approx \Omega_R$) of lower (approx. 100 cm^{-1}) frequency to represent the medium.

Fig. 1 shows plots of $\ln(W/L^2)$ vs. $\ln T$ calculated numerically for various values of the parameters E_r and ΔE. In relation to the primary photosynthetic electron transfer steps, this figure provides the following suggestions and conclusions:

(A) For processes in the normal energy gap region where $|\Delta E| < E_r$, the reactions are temperature independent for $T \lesssim T_{cr} \approx h\Omega_R/2k_B$ and follow an Arrhenius dependence at higher temperatures. This transition is smoother the broader the resonance, and when $\Gamma \approx \Omega_R$ the sharp transition observed experimentally for reactions 3 and 4 can only be reproduced if additional coupling to a narrow resonance is assumed. This was the basis of our previous analysis of reaction 3 for which good agreement with experimental data is found when $\epsilon_r(\omega)$ consists of both a broad resonance or Debye band of $\Omega_R \approx 150$ cm^{-1} and a discrete mode or a narrow resonance of $\Omega_R \approx 400$ cm^{-1} with $E_r = 1.4$ eV and $n_i = 0.9$ and 0.5, respectively [29,30]. This gave

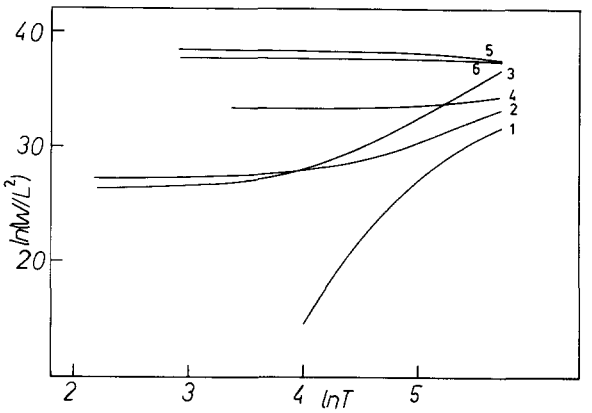

Fig. 1. Plots of $\ln(W/L^2)$ vs. $\ln T$ for a single resonance distribution. (1) $E_r = 0.5$ eV, $\Omega_R = 100$ cm^{-1}, $\Gamma = 100$ cm^{-1}, $\Delta E = 0$ (normal range). (2) Same as 1, but $\Omega_R = 400$ cm^{-1}, $\Gamma = 50$ cm^{-1}. (3) $E_r = 0.5$ eV, $\Omega_R = 100$ cm^{-1}, $\Gamma = 100$ cm^{-1}, $\Delta E = -1.0$ eV (strongly exothermic range). (4) Same as 3, but $\Omega_R = 400$ cm^{-1}, $\Gamma = 50$ cm^{-1}. (5) $E_r = 0.5$ eV, $\Omega_R = 100$ cm^{-1}, $\Gamma = 100$ cm^{-1}, $\Delta E = -0.5$ eV (activationless range). (6) Same as 5, but $\Omega_R = 400$ cm^{-1}, $\Gamma = 50$ cm^{-1}. Energy units in eV.

further an electronic coupling factor $L \approx 10^{-6}$–10^{-5} eV which is not far from the value obtained using a high-frequency single-mode approximation [27]. If we use the following expression for the electron transfer distance dependence of L suggested by Jortner [27]:

$$L = L_0 \exp(-\xi \cdot R); \quad L_0 \approx 1.25 \text{ eV}; \quad \xi \approx 1.3 \text{ Å}^{-1} \tag{20}$$

we find an electron transfer distance of $R = 9$–11 Å for reaction 3.

(B) When the energy gap coincides with E_r, a slight decrease of W with increasing T is observed, being more pronounced and beginning at lower temperatures the lower the value of Ω_R. It was noted previously [28,45] that this effect is caused by the presence of $T^{1/2}$ in the pre-exponential factor of W (Eqs. 11 and 16). It is physically associated with the inverse square-root dependence of the thermal velocity for motion on the nuclear potential surfaces. On the basis of the temperature effects it was also suggested that reactions 1, 2 and 7 belong to the activationless energy gap region [7,28,37]. The present calculation then substantiate single-mode calculations that the electronic-vibrational coupling of the donor and acceptor sites is dominated by nuclear modes of frequencies higher than 400 cm^{-1}

for the temperature-independent reactions 1 and 2, while a broader distribution of modes around 100 cm^{-1} contributes significantly for reaction 7 for which a smoother decrease of the rate constant with increasing temperature is observed experimentally. This difference may be due to the location of the primary acceptor A_1 close to the aqueous solution interphase. Using the calculated values of W for a single resonance and E_r coinciding with the energy gaps gives $L \approx 10^{-3}$ and $3 \cdot 10^{-4}$ eV for reactions 1 and 2, respectively. In terms of Eqn. 19 this gives electron transfer distances of 6 and 8 Å, respectively. For reaction 7, the very small value of $L \approx (1-2) \cdot 10^{-8}$ eV gives an electron transfer distance of 15–17 Å which is, however, a plausible value in view of the location of A_1 closer to the outside of the membrane.

(C) While the decrease of the rate constant of reaction 7 with increasing T is compatible with the behaviour expected for activationless processes, temperature independence such as that for reactions 1 and 2 would also be expected for strongly exothermic processes for which $|\Delta E| > E_r$, provided that $\Omega_R \gtrsim 400$ cm^{-1}. Lower frequency values would thus give a strong thermal activation also for strongly exothermic processes (Fig. 1). For $0.25 \lesssim E_r \lesssim 0.5$ eV, the calculations thus predict practically independence of temperature for the energy gaps of reactions 1 and 2, whereas the rate constant increases with increasing T outside this interval. For charge transfer processes in organic molecular crystals close to a crystal/solution interphase, there is in fact some evidence that E_r is about 0.3 eV [46], but for the membrane-bound redox components this quantity may be closer to the 0.4–0.5 eV suggested by the energy gaps for reactions 1 and 2 if these processes are activationless, due to the presence of polar groups and partial resolvation of the aqueous solvent.

(D) The reorganization energy of reaction 5 is presumably close to the values of reactions 1 and 2. This process then belongs to the strongly exothermic region ($|\Delta E| > E_r$), and for energy gaps of about 1 eV the weak increase of the rate constant with increasing T is compatible with frequencies about 400 cm^{-1} giving the dominating contribution and E_r in the range 0.3–0.5 eV. For smaller values a larger temperature effect is expected, and for larger values a smaller effect, unless E_r assumes unrealistically large values (greater than 1 eV).

In summary, the temperature dependence of reactions 1, 2, 5 and 7 strongly suggests that reactions 1, 2 and 7 are activationless ($\Delta E \approx -E_r$) while reaction 5 is strongly exothermic ($|\Delta E| > E_r$). Coupling to narrow distributions or discrete modes of frequencies higher than about 400 cm^{-1} is of major importance for reactions 1, 2 and 5; coupling to a broad continuum of low-frequency modes as well may also be important, but they would cause more significant temperature effects than those observed experimentally if they constitute more than 10–20% of the total reorganization energy. On the other hand, such modes do seem to provide the major part of the reorganization energy for reaction 7. Further illumination of these points, as well as the strong exothermicity effects as a possible cause for the low values of the rate constants of reactions 5 and 7 in spite of their much larger energy gaps compared with reactions 1 and 2 requires that we now proceed to a consideration of the energy gap relationships.

Free energy relationship and the effect of transmembrane potential shifts

The analysis of the temperature dependence leaves open the following questions in particular:

(1) The low rate constants of reactions 5 and 7 as compared with reactions 1 and 2 may be caused either by the much higher energy gap if these reactions are strongly exothermic, or by a larger electron-transfer distance.

(2) In the latter case, relaxation of a slow nuclear mode leading to an increased distance between $(BChl)_2^+$ and BPh^- must occur immediately subsequent to reaction 1 in order to prevent a rapid reverse electron transfer from BPh^- to $(BChl)_2^+$. A continuous distribution of nuclear modes would ensure that such slow nuclear modes are thermally activated also at cryogenic temperatures without necessarily contributing to the activation energy. Moreover, an observed relaxation time of 30 ps for a spectral shift in the $[(BChl)_2^+ + BPh]$ reaction complex has been interpreted in this way [6].

For the construction of the energy gap relation-

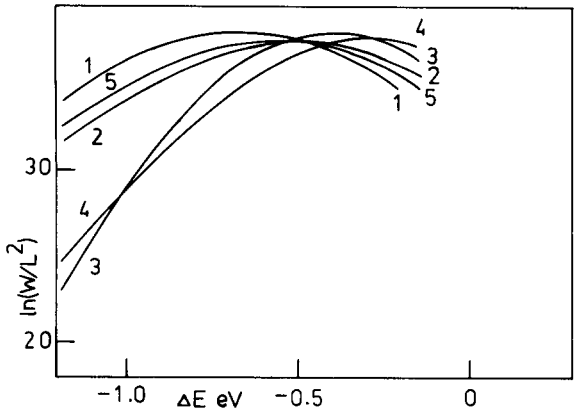

Fig. 2. Plots of $\ln(W/L^2)$ vs. ΔE. Single resonance distribution except for curve 5. $T = 298$ K. (1) $E_r = 0.5$ eV, $\Omega_R = 100$ cm^{-1}, $\Gamma = 100$ cm^{-1}. (2) Same as 1, but $\Omega_R = 400$ cm^{-1}, $\Gamma = 50$ cm^{-1} . (3) $E_r = 0.3$ eV, $\Omega_R = 100$ cm^{-1}, $\Gamma = 100$ cm^{-1}. (4) Same as 3, but $\Omega_R = 400$ cm^{-1}, $\Gamma = 80$ cm^{-1}. (5) Two resonances. $E_r = 0.5$ eV, $\Omega_{R1} = 100$ cm^{-1}, $\Gamma_1 = 100$ cm^{-1}, $\Omega_{R2} = 400$ cm^{-1}, $\Gamma_2 = 80$ cm^{-1}.

ship, we notice that Eqn. 12 has the following kinds of solution for iso- and exothermic processes [31]:

(i) When $|\Delta E| < E_r$, θ^* is located between zero and unity. In particular, $\theta^* = 0.5$ for $\Delta E = 0$. In other cases, θ^* must be found by numerical solution. θ^* coincides with the Brønsted coefficient, $\theta^* = -k_B T \mathrm{d}\ln W/\mathrm{d}\Delta E$, and for $|\Delta E| < E_r$ the rate increases with increasing (negative) ΔE.

(ii) When $\Delta E = -E_r$, $\theta^* = 0$. In this ΔE region, which in practice is quite broad (Fig. 2), there is no dependence between W and ΔE and only a weak dependence between W and the temperature.

(iii) When $|\Delta E| > E_r$, the process is strongly exothermic and $\theta^* < 0$, i.e., the rate now decreases with increasing (negative) ΔE (the inverted region).

Fig. 2 shows examples of the energy gap relationship between W and ΔE at room temperature calculated numerically by means of Eqns. 10–12. From this figure we can draw the following conclusions of importance to the primary photosynthetic electron-transfer reactions:

(1) If $E_r \approx 0.3$ eV the rate constant decreases only by a factor of 2–5 in the energy gap region 0.3–0.6 eV. The low value of the rate constant of reaction 7 is therefore almost entirely due to the larger distance for electron transfer across the membrane, and not to the more exothermic nature of this process. On the other hand, for $-\Delta E = 0.8$–1.0 eV the rate constant is lower by between 2 and 4 orders of magnitude for $E_r \approx 0.3$ eV, if $\Omega_R \lesssim 400$ cm^{-1}. The exothermicity effect is thus sufficient to explain the much lower rate constant of reaction 5 compared to those of reactions 1 and 2 for these parameter ranges. On the other hand, if the nuclear coupling is dominated by modes of frequencies at about 1000 cm^{-1} or higher, corresponding to C-C skeletal modes, the decrease is only 1 or 2 orders of magnitude. Unless other intermediates participate in the electron transfer from $(BChl)_2^*$ to BPh and A_1 [25,47–49], the low value of the rate constant of reaction 5 could therefore also be caused by relaxation of the geometry of the $[(BChl)_2^+ + BPh^-]$ pair to increase the distance between $(BChl)_2^+$ and BPh^- subsequent to the electron transfer. In terms of Eqn. 20 this increase would have to be about 2.5–4 Å to account for the observed rate decrease.

(2) For $E_r = 0.5$ eV the rate constant is again hardly changed in the ΔE range from −0.4 to −0.6 eV, and for $-\Delta E = 0.8$–1.0 eV it is lower than those of reactions 1 and 2 by no more than a factor of 50. Also in this case, it is therefore appropriate to invoke an increased electron transfer distance as a possible cause for the low rate constant of reaction 5 (cf. discussion in Ref. 50).

(3) A larger drop in the rate constant in the strongly exothermic region is predicted for lower temperatures. At 20 K, $\Delta E = -1.0$ eV and $E_r = 0.3$–0.5 eV, the rate is thus lower than at 298 K by a factor of 3–6 for $\Omega_R \approx 400$ cm^{-1} and by 10^5–10^6 for $\Omega_R \approx 100$ cm^{-1}. This effect may be part of the reason for the temperature dependence of the triplet yield in reactions 6a and 6b.

The nature of the light-induced electron-transfer processes as normal, activationless, or strongly exothermic could in principle be further illuminated by a consideration of the electrochemical potential distribution across the membrane. The free energy difference for a given electron-transfer process is thus determined not only by the electronic and equilibrium solvation energies, but also by the potential difference between the two sites. The transmembrane potential difference is subject to variation by up to several hundred millivolts by variation of ionic gradients across the membrane [51,52] or by an electric field from external macroscopic electrodes [52,53]. Provided that the potential drop varies

monotonically with the external transmembrane potential difference, a shift of the latter would furthermore be sufficient to determine the energy gap region to which a given electron-transfer process belongs without detailed knowledge of the actual potential distribution. A nonmonotonic potential distribution may, however, arise from several effects:
(i) Charge separation at the membrane/electrolyte interphase resulting from double-layer effects [54] or from lipid surface dipolar layers [56].
(ii) Discrete charge effects originating from adsorption of ions at the interphases [55] or from local electric fields caused by charged groups of membrane-bound enzymes and other 'impurities' [55].
(iii) Spatial dispersion of the membrane dielectric permittivity [57]. This arises physically from the fact that the dielectric response to an external field is correlated in space over distances comparable to the local structure. For a dielectric with a constant dielectric function (e.g., a dielectric slab between two plasma-like media such as the ionic electrolytes), spatial dispersion implies that the dielectric permittivity increases with increasing distance from the boundaries and passes a minimum at the centre, thus causing an inflection in the potential at this point [58].
(iv) Close to the interphase the free energy of an ion of charge $z_i e$ in medium 2 from the electrostatic interaction with its image charge in medium 1 is (for both dielectric and plasma-like media) [59]:

$$G_{\mathrm{im}}(x) = \frac{z_i^2 e^2}{4x\epsilon^{(2)}} \cdot \frac{\epsilon^{(2)} - \epsilon^{(1)}}{\epsilon^{(2)} + \epsilon^{(1)}} \qquad (21)$$

where x is the distance from the boundary. The ion is thus repelled from the boundary when $\epsilon^{(2)} > \epsilon^{(1)}$ (the ion in the aqueous phase) and attracted when $\epsilon^{(2)} < \epsilon^{(1)}$. When spatial dispersion is important, $\epsilon^{(k)}$ ($k = 1,2$) is replaced by $\epsilon^{(k)}(x)$, and depending on the form of this function, a nonmonotonic distribution in the membrane region may arise [60].

The relationship between a transmembrane potential shift, $\delta\Delta\psi$, and the corresponding shift in the energy gap, $\delta\Delta E$, is $\delta\Delta E = \alpha e \delta\Delta\psi$ where e is the electronic charge and $\alpha = \partial\Delta E/\partial\Delta\psi$. If $\delta\Delta\psi$ is sufficiently small that θ^* can be considered independent of ΔE, then $\delta \ln W = -\beta\theta^* \alpha e \delta\Delta\psi$. For $\alpha \approx 0.3$ ($\alpha \approx R/d$ where d is the membrane thickness if the potential drop is linear), Fig. 2 shows that for $E_r = 0.5$ eV and at room temperature an external potential shift of 200 mV causes a change of the rate constant by a factor of about 2, but in opposite directions for the normal and strongly exothermic regions, while no change is expected if $\Delta E \approx -E_r$. For $E_r = 0.3$ eV the effect is larger, amounting to factors up to 6. If coupling to low-frequency nuclear modes is of major importance, the effects are substantially larger (factors of 20–50) at low (20 K) temperatures.

External potential changes of accessible magnitude are thus expected to be detectably reflected in the variation of the rate constants, and such changes may be a useful supplement to the temperature variations in the elucidation of the nature of the membrane processes.

Acknowledgement

We would like to thank the Danish Science Research Council for financial support.

References

1 Parson, W.W. and Cogdell, R.J. (1975) Biochim. Biophys. Acta 416, 105–149
2 Dutton, P.L., Leigh, J.S., Jr., Prince, R.C. and Tiede, D.M. (1979) in Light-Induced Charge Separation in Biology and Chemistry (Gerischer, H. and Katz, J.J., eds.), pp. 411–448, Verlag-Chemie, New York
3 DeVault, D.C. (1980) Q. Rev. Biophys., in the press
4 Netzel, T.L., Rentzepis, P.M. and Leigh, J.S. (1975) Science 182, 238–241
5 Fajer, J., Brune, D.C., Davis, M.S., Forman, A. and Spaulding, L.D. (1975) Proc. Natl. Acad. Sci. U.S.A. 72, 4956–4960
6 Rockley, M.G., Windsor, M.W., Cogdell, R.J. and Parson, W.W. (1975) Proc. Natl. Acad. Sci. U.S.A. 72, 2251–2255
7 Peters, K., Avouris, P. and Rentzepis, P.M. (1978) Biophys. J. 23, 207–217
8 DeVault, D.C. and Chance, B. (1966) Biophys. J. 6, 825–847
9 Parson, W.W. (1967) Biochim. Biophys. Acta 131, 154–172
10 Clayton, R.K. and Yau, H.F. (1972) Biophys. J. 12, 867–881
11 Hsi, E.S.P. and Bolton, J.R. (1974) Biochim. Biophys. Acta 347, 126–133
12 McElroy, J.D., Mauzerall, D.C. and Feher, G. (1974) Biochim. Biophys. Acta 333, 261–277
13 Loach, P.A., Kung, M.C. and Hales, B.J. (1975) Ann. N.Y. Acad. Sci. 244, 297–319

14 Morrison, L.E. and Loach, P.A. (1978) Photochem. Photobiol. 27, 751–757
15 Case, G.D. and Parson, W.W. (1971) Biochim. Biophys. Acta 253, 187–202
16 Chamorovskij, S.K., Remennikov, S.M., Kononenko, A.A., Venediktov, P.S. and Rubin, A.B. (1976) Biochim. Biophys. Acta 430, 62–70
17 Parak, F., Frolov, E.N., Kononenko, A.A., Mössbauer, R.L., Gol'danskij, V.I. and Rubin, A.B. (1980) FEBS Lett. 117, 368–372
18 Crofts, A.R. (1979) in Light-Induced Charge Separation in Chemistry and Biology (Gerischer, H. and Katz, J.J., eds.), pp. 389–410, Verlag-Chemie, New York
19 Parson, W.W., Clayton, R.K. and Cogdell, R.J. (1975) Biochim. Biophys. Acta 387, 265–278
20 Blankenship, R.E. and Parson, W.W. (1978) in Photosynthesis in Relation to Model System (Barber, J., ed.) Elsevier, Amsterdam
21 Haberkorn, R. and Micel-Beyerle, M.E. (1977) FEBS Letters 75, 5–8
22 Michel-Beyerle, M.E., Scheer, H., Seidlitz, H., Tempus, D. and Haberkorn, R. (1979) FEBS Letters 100, 9–12
23 Haberkorn, R. and Michel-Beyerle, M.E. (1979) Biophys. J. 26, 489–498
24 Müller, N., Papier, G., Charlé, K.-P. and Willig, F. (1979) Ber. Bunsenges. Phys. Chem. 83, 130–140
25 Haberkorn, R., Michel-Beyerle, M.E. and Marcus, R.A. (1979) Proc. Nat. Acad. Sci. USA 76, 4185–4188
26 Hopfield, J.J. (1974) Proc. Natl. Acad. Sci. USA 71, 3640–3644
27 Jortner, J. (1976) J. Chem. Phys. 64, 4860–4867
28 Bukhs, E. and Jortner, J. (1980) FEBS Letters 109, 117–120
29 Kuznetsov, A.M., Søndergård, N.C. and Ulstrup, J. (1978) Chem. Phys. 29, 383–390
30 Dogonadze, R.R., Kuznetsov, A.M., Zakaraya, M.G. and Ulstrup, J. (1979) in: Tunnelling in Biological Systems (Chance, B., DeVault, D.C., Frauenfelder, H., Marcus, R.A., Schrieffer, J.R. and Sutin, N., eds.), pp. 145–171, Academic Press, New York
31 Dogonadze, R.R., Kuznetsov, A.M., Vorotyntsev, M.A. and Zakaraya, M.G. (1977) J. Electroanal. Chem. 75, 315–331
32 Perlin, Yu. I. (1964) Usp. Fiz. Nauk 80, 553–595
33 Dogonadze, R.R. and Kuznetsov, A.M. (1973) Physical Chemistry, Kinetics, VINITI, Moscow
34 Dogonadze, R.R. and Kuznetsov, A.M. (1975) Progr. Surf. Sci. 6, 1–42
35 Dogonadze, R.R. and Kuznetsov, A.M. (1978) Kinetics and Catalysis, VINITI, Moscow
36 Kestner, N.R., Logan, J. and Jortner, J. (1974) J. Phys. Chem. 78, 2148–2166
37 Ulstrup, J. (1979) Charge Transfer Processes in Condensed Media, Lecture Notes in Chemistry, Vol. 10, Springer-Verlag, Berlin
38 Lax, M. (1952) J. Chem. Phys. 20, 1752–1760
39 Levich, V.G. and Dogonadze, R.R. (1961) Collect. Czech. Chem. Commun. 26, 193–214
40 Lang, I.G. and Firsov, Yu. A. (1963) Sov. Phys. JETP 16, 1301–1312
41 Jortner, J. and Ulstrup, J. (1979) Chem. Phys. Lett. 63, 236–239
42 Fröhlich, H. (1952) Theory of Dielectrics, 2nd edn., Clarendon, Oxford
43 Saxton, R. (1952) Proc. R. Soc. A213, 473–490
44 Afsar, M.N. and Hasted, J.B. (1979) Infrared Phys. 18, 835–843
45 Sarai, A. (1979) Chem. Phys. Lett. 63, 360–365
46 Eichhorn, M. and Willig, F. (1980) Proceedings of the 31st Meeting of the International Society of Electrochemistry (Vecchi, E., ed.), pp. 554–555, Venice
47 Shuvalov, V.A., Klevanik, A.V., Sharkov, A.V., Matveets, L.A. and Krukov, P.G. (1978) FEBS Lett. 91, 135–139
48 Shuvalov, V.A. and Asadov, A.A. (1979) Biochim. Biophys. Acta 545, 296–308
49 Palliotin, G., Vermeglio, A. and Breton, J. (1979) Biochim. Biophys. Acta 545, 249–264
50 Vorotyntsev, M.A. and Itskovich, E.M. (1980) J. Theor. Biol. 86, 223–236
51 Takamiya, K. and Dutton, P.L. (1977) FEBS Lett. 80, 279–284
52 Witt, H.T. (1978) Biochim. Biophys. Acta 505, 355–427
53 Witt, H.T., Schlodder, E. and Gräber, P. (1976) FEBS Lett. 69, 272–276
54 McLaughlin, S. (1977) Curr. Top. Membranes Transp. 9, 71–144
55 Sackmann, E. (1979) in Light-Induced Charge Separation in Biology and Chemistry (Gerischer, H. and Katz, J.J., eds.), pp. 259–284, Verlag-Chemie, New York
56 Nelson, A.P. and McQuarrie, D.A. (1975) J. Theor. Biol. 55, 13–27
57 Dogonadze, R.R. and Kornyshev, A.A. (1974) J.C.S. Faraday Trans. II 70, 1121–1131
58 Kornyshev, A.A., Ulstrup, J. and Vorotyntsev, M.A. (1981) Thin Solid Films 75, 105–118
59 Landau, L.D. and Lifshitz, E.M. (1975) Electrodynamics of Continuous Media, 3rd ed., Pergamon Press, Oxford
60 Kornyshev, A.A., Rubinshtein, A.I. and Vorotyntsev, M.A. (1977) Phys. Status Solidi 84 (b), 125–132